

RESEARCH

Open Access



Knockdown of circ_0003928 ameliorates high glucose-induced dysfunction of human tubular epithelial cells through the miR-506-3p/HDAC4 pathway in diabetic nephropathy

Qiong Liu¹, Yuanyuan Cui², Nan Ding³ and Changxue Zhou^{4*}

Abstract

Background: Previous data have indicated the importance of circular RNA (circRNA) in the pathogenesis of diabetic nephropathy (DN). The study is designed to investigate the effects of circ_0003928 on oxidative stress and apoptosis of high glucose (HG)-treated human tubular epithelial cells (HK-2) and the underlying mechanism.

Methods: The DN cell model was established by inducing HK-2 cells using 30 mmol/L D-glucose. RNA expression of circ_0003928, miR-506-3p and histone deacetylase 4 (HDAC4) was detected by quantitative real-time polymerase chain reaction. Cell viability and proliferation were investigated by cell counting kit-8 and 5-Ethynyl-29-deoxyuridine (EdU) assays, respectively. Oxidative stress was evaluated by commercial kits. Caspase 3 activity and cell apoptotic rate were assessed by a caspase 3 activity assay and flow cytometry analysis, respectively. Protein expression was detected by Western blotting analysis. The interactions among circ_0003928, miR-506-3p and HDAC4 were identified by dual-luciferase reporter and RNA pull-down assays.

Results: Circ_0003928 and HDAC4 expression were significantly upregulated, while miR-506-3p was downregulated in the serum of DN patients and HG-induced HK-2 cells. HG treatment inhibited HK-2 cell proliferation, but induced oxidative stress and cell apoptosis; however, these effects were reversed after circ_0003928 depletion. Circ_0003928 acted as a miR-506-3p sponge, and HDAC4 was identified as a target gene of miR-506-3p. Moreover, the circ_0003928/miR-506-3p/HDAC4 axis regulated HG-induced HK-2 cell dysfunction.

Conclusion: Circ_0003928 acted as a sponge for miR-506-3p to regulate HG-induced oxidative stress and apoptosis of HK-2 cells through HDAC4, which suggested that circ_0003928 might be helpful in the therapy of DN.

Keywords: DN, circ_0003928, miR-506-3p, HDAC4

Introduction

Diabetic nephropathy (DN) is the primary inducer of end-stage renal disease and is a serious complication of diabetes, featured by persistent microalbuminuria, increased blood pressure and decreased

glomerular filtration rates [1]. The most significant pathological changes for DN patients are the glomerular lesions (mesangial expansion and glomerular basement membrane thickening) [2]. Besides, hyperglycemia induces oxidative stress and apoptosis of tubular epithelial cells in DN [3, 4]. At present, the multipronged drug approach by reducing proteinuria under control fails to fully prevent DN development. Thus, an in-depth investigation of the molecular mechanism related to oxidative

*Correspondence: changxuezhou@163.com

⁴ Department of Kidney Internal Medicine, Zaozhuang Municipal Hospital, No. 41 Longtou Road, Central District, Zaozhuang 277100, China
Full list of author information is available at the end of the article



© The Author(s) 2022. **Open Access** This article is licensed under a Creative Commons Attribution 4.0 International License, which permits use, sharing, adaptation, distribution and reproduction in any medium or format, as long as you give appropriate credit to the original author(s) and the source, provide a link to the Creative Commons licence, and indicate if changes were made. The images or other third party material in this article are included in the article's Creative Commons licence, unless indicated otherwise in a credit line to the material. If material is not included in the article's Creative Commons licence and your intended use is not permitted by statutory regulation or exceeds the permitted use, you will need to obtain permission directly from the copyright holder. To view a copy of this licence, visit <http://creativecommons.org/licenses/by/4.0/>. The Creative Commons Public Domain Dedication waiver (<http://creativecommons.org/publicdomain/zero/1.0/>) applies to the data made available in this article, unless otherwise stated in a credit line to the data.

stress and apoptosis of tubular epithelial cells in DN is required for the development of new therapeutic targets.

Circular RNA is a new member of noncoding RNAs and forms a loop through a specific event called head-to-tail splicing [5]. Owing to its wide expression in various types of cells, circRNA is attracting the attention of most investigators in revealing the pathogenesis of human diseases [6]. CircRNA governs gene expression by serving as a chelator of RNA-binding protein, a sponge for microRNA (miRNA) or a regulator of nuclear transcription [7]. Recently, research data have indicated the involvement of circRNA in renal diseases, such as renal cell carcinoma, lupus nephritis, and DN [8]. Emerging evidence indicates the function of circRNA in DN. For example, circ_010383 inhibited miR-135a to regulate renal fibrosis in DN [9]. Circ_0000064 combined with miR-143 to regulate the proliferation and fibrosis of mesangial cells in DN [10]. Circ_0003928, formed by back-splicing of TAO kinase 1 (TAOK1) gene, is one of 10 upregulated circRNAs in high glucose-induced human umbilical vein endothelial cells [11], suggesting that circ_0003928 may be involved in the pathogenesis of DN. However, the reports about the mechanism underlying circ_0003928 regulating DN development are still lacking.

miRNA, 18–25 nucleotides in length, is a noncoding single-stranded RNA that regulates gene expression post-transcriptionally [12]. miRNA regulates different biological behaviors of cells, such as cell differentiation, division, and apoptosis, thereby being involved in the pathogenesis of disease development [12]. Previous evidence has suggested the pathogenesis of DN involves some miRNAs, such as miR-342 [13], miR-337 [14] and miR-34a-5p [15]. Given that circRNA can competitively combine with miRNA through miRNA response elements to regulate the expression of the miRNA target mRNA [16], we try to assemble a circ_0003928–miRNA–mRNA regulatory axis to explain the underlying mechanism of circ_0003928 in DN development.

Thus, we hypothesized that circ_0003928 regulated DN progression through circ_0003928–miRNA–mRNA axis. The present study analyzed circ_0003928 expression in the serum of DN patients and high glucose (HG)-treated human tubular epithelial cells, investigated the effects of circ_0003928 on HG-triggered tubular epithelial cell damage, and determined a regulatory mechanism of circ_0003928 in DN development.

Materials and methods

Serum samples

Serum samples were collected from 41 DN patients (gender: 20 male and 21 female; age: 56.4 ± 6.2) and 29 healthy volunteers (gender: 17 male and 12 female; age: 57.3 ± 5.6) in Hebei General Hospital. The diagnosis of

diabetic nephropathy was performed by two experienced renal pathologists. All serum samples were obtained by centrifugation at 3000 rpm for 10 min, and stored at -80°C for subsequent RNA extraction. The clinical trial obtained approval from the Ethics Committee of Hebei General Hospital (approval number 2020NYH Y-010–04). All participants signed the written informed consent.

Cell culture and DN cell model

Human tubular epithelial cells (HK-2) were purchased from Procell (Wuhan, China), and cultured in Dulbecco's modified Eagle's medium (DMEM; Procell) added with 10% fetal bovine serum (FBS; Procell) and 1% penicillin/streptomycin (Procell) at 37°C in an atmosphere of 5% CO_2 . According to the reported method [17, 18], the DN cell model was established by treating HK-2 cells with 30 mmol/L D-glucose (HG; MedChemExpress, Shanghai, China), with 5 mmol/L D-glucose (NG; MedChemExpress) and 30 mmol/L Mannitol (MedChemExpress) acting as controls.

Quantitative real-time polymerase chain reaction (qRT-PCR)

Total RNA from HK-2 cells was extracted using TsingZol (Tsingke, Shanghai, China). RNA quality was measured by detecting the A260/A280 ratio on NanoDrop-1000 apparatus. 2 μg RNA and 100 nm mRNA were reversely transcribed to cDNA using Goldenstar™ RT6 cDNA Synthesis Mix (Tsingke), gDNA remover (Tsingke) and RNasin (Tsingke). 5 μg miRNA was reversely transcribed to cDNA using miRNA synthesis reagents (TaKaRa, Dalian, China), including mRQ Buffer, mRQ Enzyme and RNase I as instructed. Then, qRT-PCR was performed to detect gene expression using T5 Fast qPCR Mix (Tsingke). In brief, 50 ng cDNA was mixed with 10 μL T5 Fast qPCR Mix (SYBR Green), 0.8 μL primers and 0.4 μL ROX Reference Dye, and reacted at 95°C for 1 min, and 40 cycles at 95°C for 10 s and 60°C for 10 s on an Applied Biosystems. The $2^{-\Delta\Delta\text{Ct}}$ method was used to calculate gene expression with glyceraldehyde 3-phosphate dehydrogenase (GAPDH) [19] and U6 as internal controls. The primer sequences are listed in Table 1.

Cell transfection

The small interfering RNA against circ_0003928 (si-circ_0003928, 5'-AAGAGGATGGCCCCAGAAGTA-3'), the mimics of miR-506-3p (miR-506-3p, 5'-UAAGGCACCCUUCUGAGUAGA-3'), the inhibitors of miR-506-3p (anti-miR-506-3p, 5'-UCUACUCAGAAGGGU GCCUUA-3'), and respective controls, including siRNA negative control (si-NC), the negative control of miRNA mimics (miR-NC) and the negative control of miRNA inhibitors (anti-miR-NC) were synthesized in Ribobio

Table 1 Primers sequences used for qRT-PCR

Name		Sequences (5'-3')
circ_0003928	Forward	CCCAACAGAAGAAAGAAC
	Reverse	CTTTGCCATCATATTGTC
HDAC4	Forward	AGCAGAGGTTGAGCGTGAG
	Reverse	GAAGTTCCCATCGTCGTAG
miR-506-3p	Forward	ACACTCATAAGGCACCCTTC
	Reverse	TCTACTCAGAAGGGGAGTAC
GAPDH	Forward	CAAATTCATGGCACCGTCA
	Reverse	GACTCCACGACGTACTIONCAGC
U6	Forward	CTTCGGCAGCACATATACT
	Reverse	AAAATATGGAACGCTTCACG

Co., Ltd. (Guangzhou, China). The open reading frame of HDAC4 was amplified and then inserted into the pcDNA 3.1 vector by GenePharma Co., Ltd. (Shanghai, China) to generate the overexpression plasmid of HDAC4 (HDAC4). Then, cell transfection was performed on HK-2 cells in accordance with the manufacturer's direction of FuGENE6 (Roche, Basel, Switzerland).

Analysis of cell viability

To analyze cell viability, HK-2 cells treated with mannitol, normal glucose (NG), HG, plasmids, small RNA or small interfering RNA were cultured in 96-well plates for 48 h. Then, the cell counting kit-8 (CCK-8) reagent (Beyotime, Shanghai, China) was added to each well of these plates. After 4 h of incubation, these samples were analyzed using a microporous plate spectrophotometer (Bio-Rad, Hercules, CA, USA) with a wavelength of 450 nm.

5-Ethynyl-29-deoxyuridine (EdU) assay

After various treatments as mentioned above, HK-2 cells were cultured in 6-well plates for 48 h. Afterward, the cells were sub-cultured in the 96-well plates added with EdU-labeled DMEM at 37 °C for 2 h. Subsequent experiments were conducted according to the instruction of the EdU staining kit (Ribobio). Finally, cell proliferation was determined by analyzing EdU-positive cells using a fluorescence microscope (Olympus, Tokyo, Japan).

Analysis of oxidative stress

The assay regarding the detection of reactive oxygen species (ROS), malondialdehyde (MDA) and superoxide dismutase (SOD) levels was performed to evaluate oxidative stress. In brief, 2×10^6 HK-2 cells for each experiment were harvested, and subsequent procedures were carried out following the instruction of the cellular ROS assay kit (Abcam, Cambridge, MA, USA), lipid peroxidation MDA assay kit (Abcam), and SOD activity assay kit (Abcam).

Finally, the outputs of these samples were measured by a microporous plate spectrophotometer (Bio-Rad).

Detection of caspase 3 activity

HK-2 cells were harvested and lysed using lysis buffer (Beyotime). The cells were centrifuged at 18,000 g for 12 min, and then cell supernatant was collected. These samples were incubated with Ac-DEVD-pNA (Beyotime), and caspase 3 activity was detected using a microplate reader (Bio-Rad).

Flow cytometry analysis

After various treatments, HK-2 cells were cultured in 12-well plates for 48 h. These cells were harvested by centrifuging and then suspended in Binding buffer (Solarbio, Beijing, China), followed by incubating with Annexin V-FITC (Solarbio) and propidium iodide (Solarbio). At last, the stained cells were analyzed using a flow cytometer (Thermo Fisher, Waltham, MA, USA).

Western blotting

Concisely, cells and tissues were incubated with Protein Extraction Reagent (Phygene, Fuzhou, China) containing Protease Inhibitor Cocktail for 20 min on ice, and total proteins were extracted by centrifugation at 10,000g for 20 min. Then, 20 µg of protein were loaded onto 8%-12% bis-tris-acrylamide gels (Phygene). The proteins were wet-transferred onto nitrocellulose membranes, which were then blocked with 5% defatted dry milk. Next, the primary antibodies specific to BCL2-associated x protein (Bax; 1:1000; Thermo Fisher), cleaved caspase 3 (1:1500; Thermo Fisher), B-cell lymphoma-2 (Bcl 2; 1:50; Thermo Fisher), HDAC4 (1:1500; Thermo Fisher) and GAPDH (1:1000; Thermo Fisher) were used to incubate the membranes. After being probed with secondary antibodies (Thermo Fisher), the membranes were analyzed under a Bio-Rad image analysis system with the use of eyoECL Plus (Beyotime).

Dual-luciferase reporter assay

Online database starbase (<http://starbase.sysu.edu.cn/agoClipRNA.php?source=mRNA>) was employed for the prediction of potential regulatory relationships among circ_0003928, miR-506-3p and HDAC4. Then, circ_0003928 and HDAC4 3'UTR sequences harboring the complementary sites of miR-506-3p were amplified by qRT-PCR and introduced into the pmirGLO vector to construct wild-type (WT) reporter plasmids, including circ_0003928-WT and HDAC4-3'UTR-WT. Similarly, the mutant (MUT) plasmids, including circ_0003928-MUT and HDAC4-3'UTR-MUT, were assembled. As instructed [20], cell transfection was performed on HK-2 cells with the use of the reporter

plasmids, miRNA mimics, miRNA negative controls and transfection reagents. After 48 h of cell transfection, the cells were harvested for the detection of luciferase activity using a Dual-Lucy assay kit (Solarbio).

RNA pull-down assay

The HK-2 cells cultured in 12-well plates were treated with biotin-labeled miR-506-3p mimics (Bio-miR-506-3p) and Bio-miR-NC alone. After 48 h of culture, these cells were lysed using RIP lysis buffer. After that, the supernatant was collected and incubated with streptavidin-coupled beads (Sigma, St. Louis, MO, USA). At last, circ_0003928 level in the co-precipitated RNAs was analyzed by qRT-PCR.

Statistical analysis

All data were obtained from three independent duplicate tests and analyzed by GraphPad Prism software. Results were shown as means ± standard deviations (SD). Significant differences were compared with Mann–Whitney *U* test, Student’s *t*-tests, or analysis of variance. *P* < 0.05 indicated statistical significance.

Results

HG treatment induced circ_0003928 expression in HK-2 cells

Circ_0003928 is located in chr17:27,809,241–27,838,010 and generated by the cyclization of exons 8–15 of the TAOK1 gene (Fig. 1A). Meanwhile, the data from qRT-PCR showed the high expression of circ_0003928 in HG-induced HK-2 cells as compared with normal glucose (NG) or mannitol-induced HK-2 cells (Fig. 1B). The above results suggest that the pathogenesis of DN may be associated with circ_0003928.

HG treatment inhibited HK-2 cell proliferation but induced oxidative stress and cell apoptosis

HK-2 cells were treated with 30 mmol/L D-glucose to simulate a DN cell model in vitro, regarding 5 mmol/L D-glucose and 30 mmol/L Mannitol as controls. Subsequently, we analyzed the effects of HG treatment on HK-2 cell proliferation, oxidative stress and cell apoptosis using the model. As displayed in Fig. 2A and B, HG treatment inhibited cell viability and cell proliferation in comparison with control groups. Besides, oxidative stress was induced after HG treatment in HK-2 cells. For instance, ROS and MDA levels were increased, and SOD activity was inhibited after HG treatment (Fig. 2C–E).

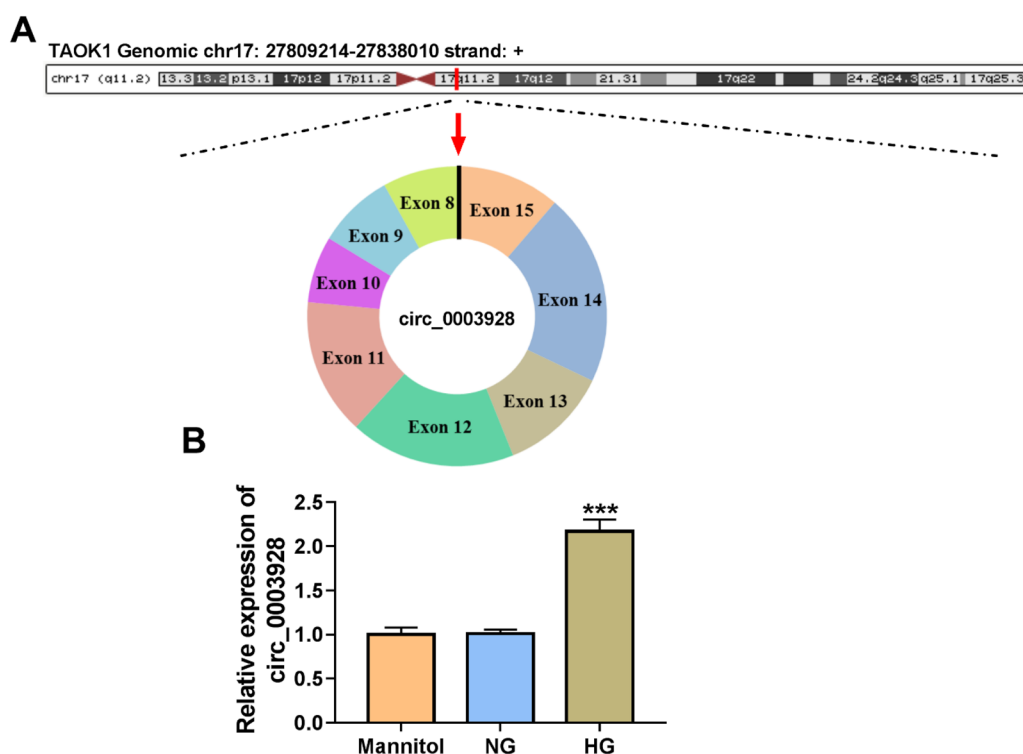


Fig. 1 The expression of circ_0003928 in serum samples of DN patients and HG-induced HK-2 cells. **A** The schematic diagram showed the formation of circ_0003928. **B** Circ_0003928 expression was detected by qRT-PCR in the HK-2 cells induced by mannitol, NG or HG. ****P* < 0.001

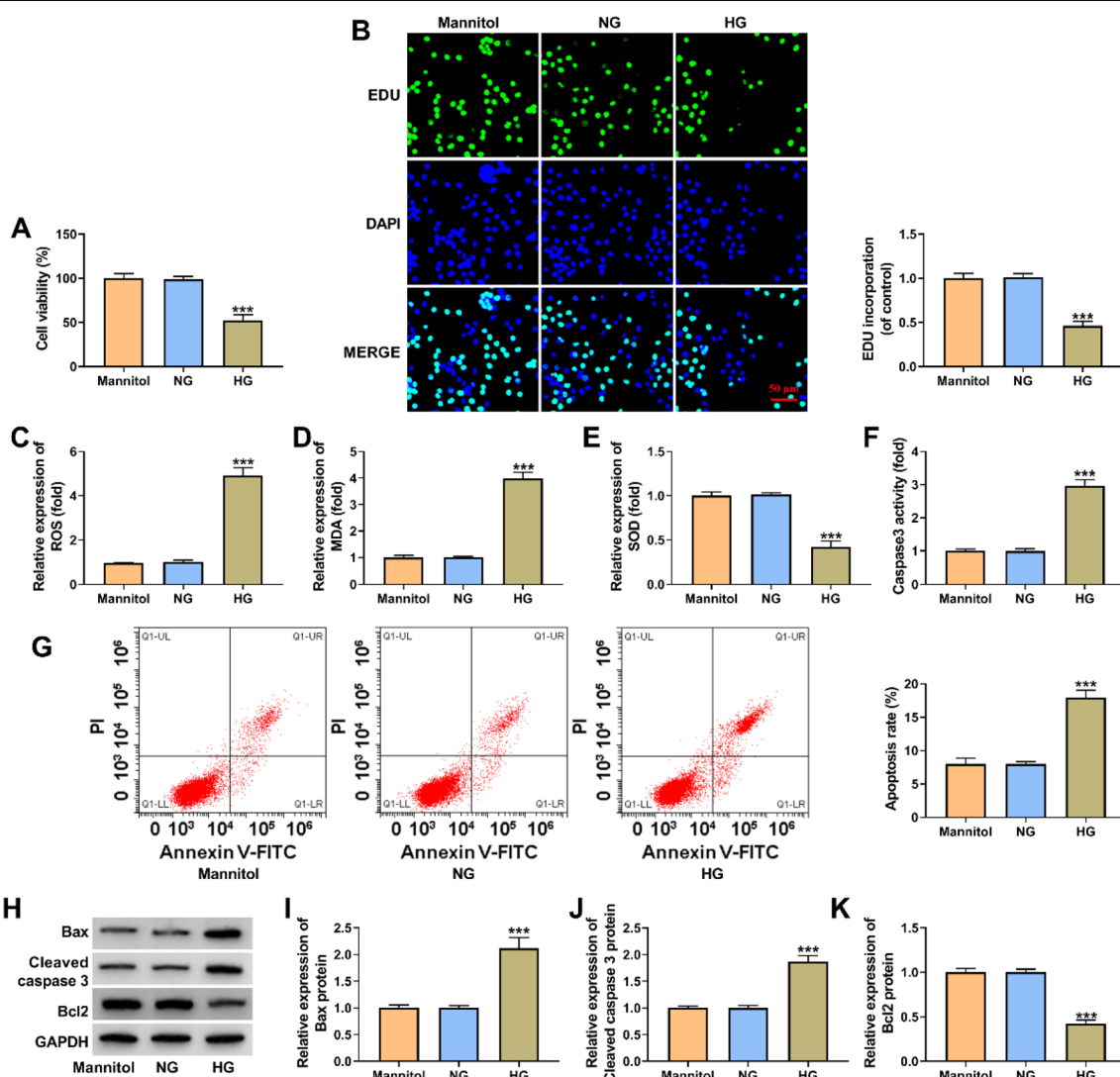


Fig. 2 The effects of HG treatment on HK-2 cell proliferation, oxidative stress and apoptosis. A-K HK-2 cells were treated with 30 mmol/L D-glucose, 5 mmol/L D-glucose and 30 mmol/L Mannitol, respectively, and cell viability was analyzed by a CCK-8 assay (A), cell proliferation by an EdU assay (B), ROS level by a cellular ROS assay kit (C), MDA production by a lipid peroxidation MDA assay kit (D), SOD activity by a Superoxide dismutase activity assay kit (E), caspase 3 activity by a caspase 3 activity assay (F), cell apoptotic rate by flow cytometry analysis (G), and the protein expression of Bax, cleaved caspase 3 and Bcl 2 by Western blotting analysis (H-K). *** $P < 0.001$

Comparatively, HG treatment increased caspase 3 activity and induced HK-2 cell apoptosis, accompanied by the increases of Bax and cleaved caspase 3 expression and a decrease of Bcl 2 expression (Fig. 2F–K). Collectively, the above evidence suggests the successful establishment of the DN cell model.

Circ_0003928 depletion assuaged high glucose (HG)-induced oxidative stress and apoptosis of HK-2 cells

We depleted circ_0003928 in HG-induced HK-2 cells to determine the consequential effects on cell proliferation, oxidative stress and cell apoptosis. The data from Fig. 3A

first showed that HG-increased circ_0003928 expression was attenuated after circ_0003928 knockdown. Subsequently, HG-induced inhibition of cell viability and cell proliferation were relieved when circ_0003928 expression was decreased (Fig. 3B and C). HG treatment led to increases in OS and MDA levels and a decrease in SOD activity; however, these effects were attenuated after transfection with si-circ_0003928 (Fig. 3D–F). Comparatively, the increased caspase 3 activity and cell apoptotic rate by HG treatment were rescued after circ_0003928 depletion (Fig. 3G and H). Further, knock-down of circ_0003928 remitted HG treatment-triggered

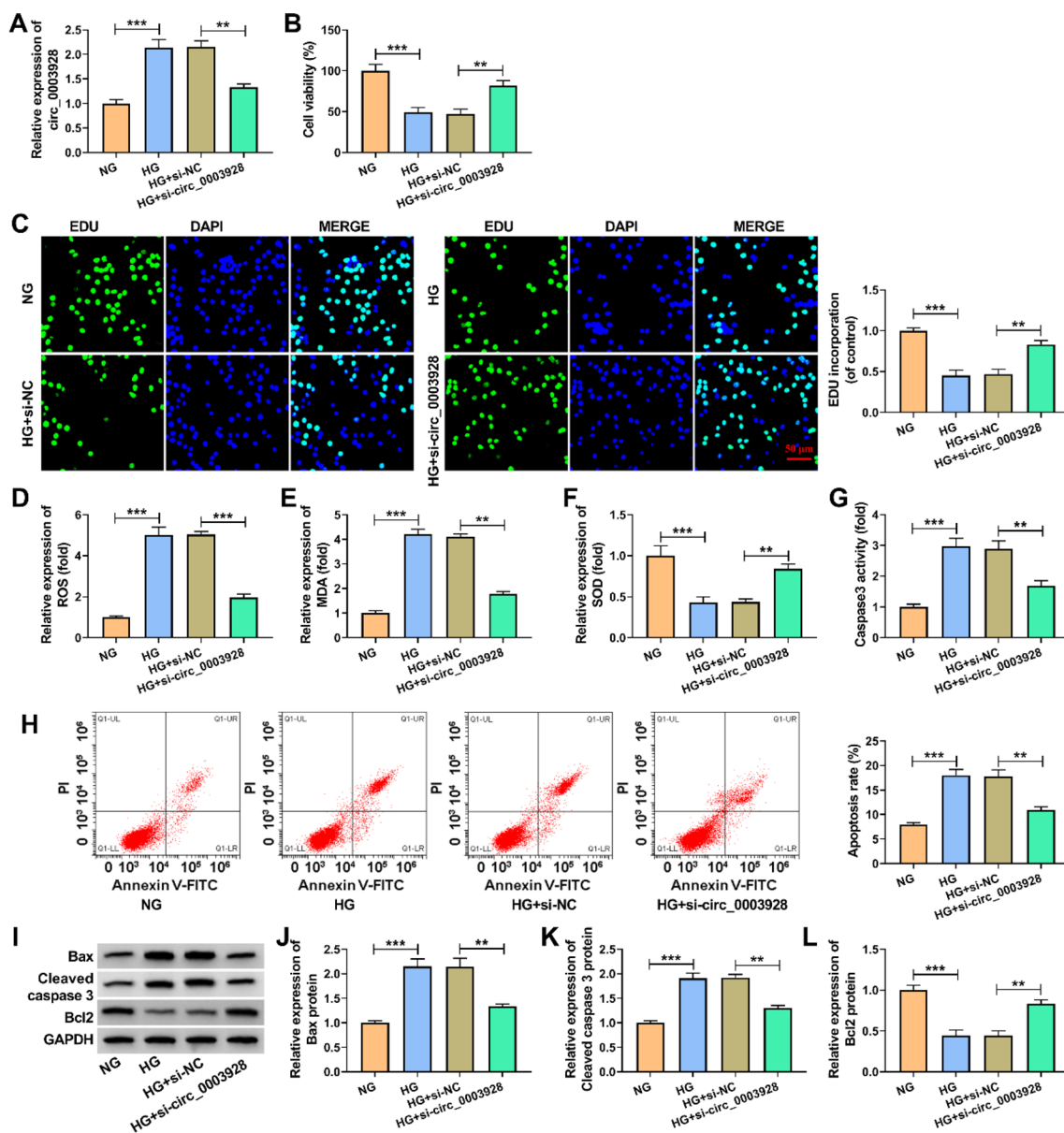


Fig. 3 The effect of circ_0003928 depletion on HG-induced HK-2 cell damage. **A–L** HK-2 cells were treated with NG, HG, HG + si-NC and HG + si-circ_0003928, respectively, and circ_0003928 expression was analyzed by qRT-PCR (**A**), cell viability by a CCK-8 assay (**B**), cell proliferation by an EdU assay (**C**), ROS level by a cellular ROS assay kit (**D**), MDA production by a lipid peroxidation MDA assay kit (**E**), SOD activity by a Superoxide dismutase activity assay kit (**F**), caspase 3 activity by a caspase 3 activity assay (**G**), cell apoptotic rate by flow cytometry analysis (**H**), and the protein expression of Bax, cleaved caspase 3 and Bcl 2 by Western blotting analysis (**I–L**). ** $P < 0.01$ and *** $P < 0.001$

dysregulation of Bax, cleaved caspase 3 and Bcl 2 expression (Fig. 3I–L). Therefore, these findings demonstrate that circ_0003928 can regulate HG-induced oxidative stress and apoptosis of HK-2 cells.

Circ_0003928 acted as a miR-506-3p sponge

Starbase online database was employed to predict the possible target miRNAs of circ_0003928. In this

study, we analyzed 4 miRNAs that not only contained circ_0003928-binding sites, but also inhibited DN progression, including miR-142-3p, miR-205-5p, miR-31-5p and miR-506-3p. qRT-PCR first showed that circ_0003928 depletion increased the expression of miR-142-3p and miR-506-3p, especially miR-506-3p, but it had no significant difference in miR-205-5p and miR-31-5p expression (Additional file 1: Figure S1A).

Thus, miR-506-3p was chosen as a follow-up study. As presented in Fig. 4A, miR-506-3p contained the binding sites of circ_0003928, suggesting the potential interaction between circ_0003928 and miR-506-3p. Consistently, the data from the qRT-PCR analysis showed that miR-506-3p was significantly downregulated in HG-treated HK-2 cells compared with its expression in the HK-2 cells treated with mannitol or NG (Fig. 4B). Our data confirmed the interaction of circ_0003928 with miR-506-3p. For instance, miR-506-3p overexpression significantly inhibited the luciferase activity of wild-type reporter plasmid of circ_0003928 rather than that of the mutant reporter plasmid, as shown in Fig. 4C. Meanwhile, biotin-labeled miR-506-3p could greatly enrich circ_0003928 in comparison with biotin-labeled miR-NC, as analyzed by RNA pull-down assay (Fig. 4D). Further, circ_0003924 expression was negatively correlated with miR-506-3p in the blood samples of DN patients (Additional file 2: Figure S2A). Taken together, the above evidence demonstrates that circ_0003928 binds to miR-506-3p.

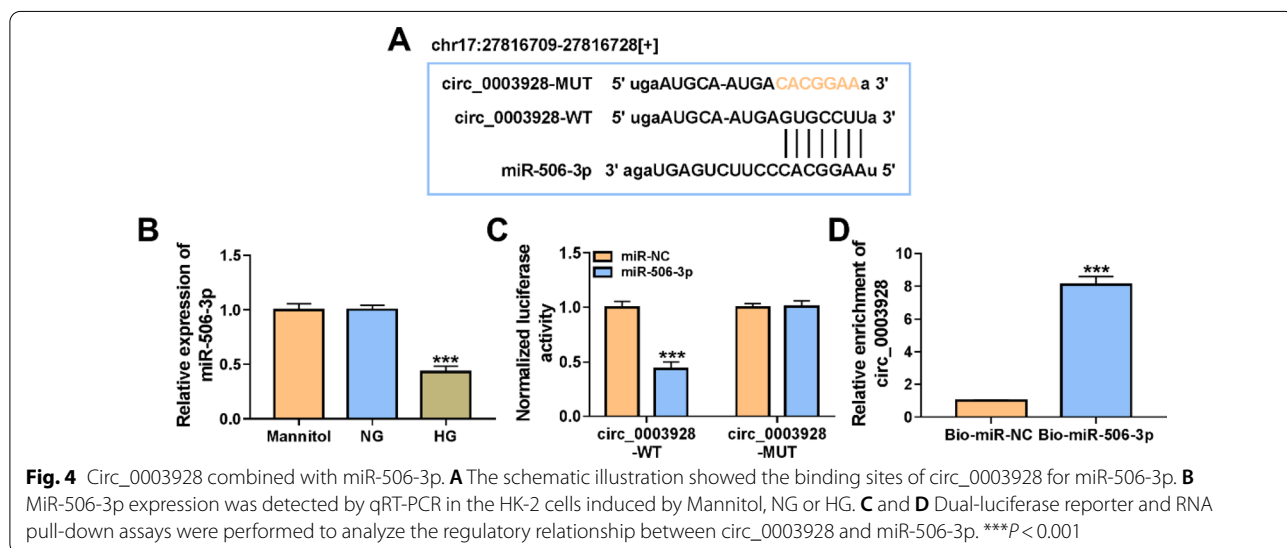
Circ_0003928 regulated HG-induced oxidative stress and apoptosis of HK-2 cells through miR-506-3p

Given the regulatory relationship between circ_0003928 and miR-506-3p, the study continued to analyze whether miR-506-3p participated in the regulation of circ_0003928 toward HG-induced HK-2 cell damage. To this end, we transfected si-circ_0003928, anti-miR-506-3p and matched controls into HG-induced HK-2 cells. Figure 5A first showed that HG-induced inhibition of miR-506-3p expression was enhanced after transfection with anti-miR-506-3p, showing the high efficiency of miR-506-3p knockdown. Then, circ_0003928 knockdown-induced increases of cell viability and cell

proliferation were relieved after miR-506-3p knockdown under HG treatment (Fig. 5B and C). Besides, knockdown of circ_0003928 led to decreased ROS and MDA production and increased SOD activity in HG-induced HK-2 cells, but these effects were remitted when miR-506-3p expression was reduced (Fig. 5D–F). Similarly, circ_0003928 depletion decreased caspase 3 activity, cell apoptotic rate and the protein expression of Bax and cleaved caspase 3, and increased Bcl 2 expression; however, these effects were remitted after miR-506-3p depletion (Fig. 5G–L). Collectively, these findings demonstrate that the circ_0003928/miR-506-3p axis is involved in HG-induced HK-2 cell injury.

Circ_0003928 mediated HDAC4 expression by interacting with miR-506-3p

We further identified miR-506-3p-associated mRNAs. SOX6, CDKN1A, ROCK1, NFAT5, ICAM1 and HDAC4 were chosen for subsequent studies as these mRNAs potentially bound to miR-506-3p and contributed to DN progression. By qRT-PCR analysis, we found that miR-506-3p also affected (downregulated) the expression of ROCK1 and HDAC4, especially HDAC4, among these mRNAs (Additional file 1: Figure S1B). Thus, HDAC4 was employed in the following study. HDAC4 containing the potential binding sites of miR-506-3p (Fig. 6A), as predicted by the starbase online database, was selected for the subsequent study. The study first showed a significantly high expression of HDAC4 in HG-induced HK-2 cells, as compared with control groups (Fig. 6B and C). Subsequently, we found that miR-506-3p mimics significantly reduced the luciferase activity of wild-type reporter plasmid of HDAC4 3’UTR, but that of mutant reporter plasmid had no



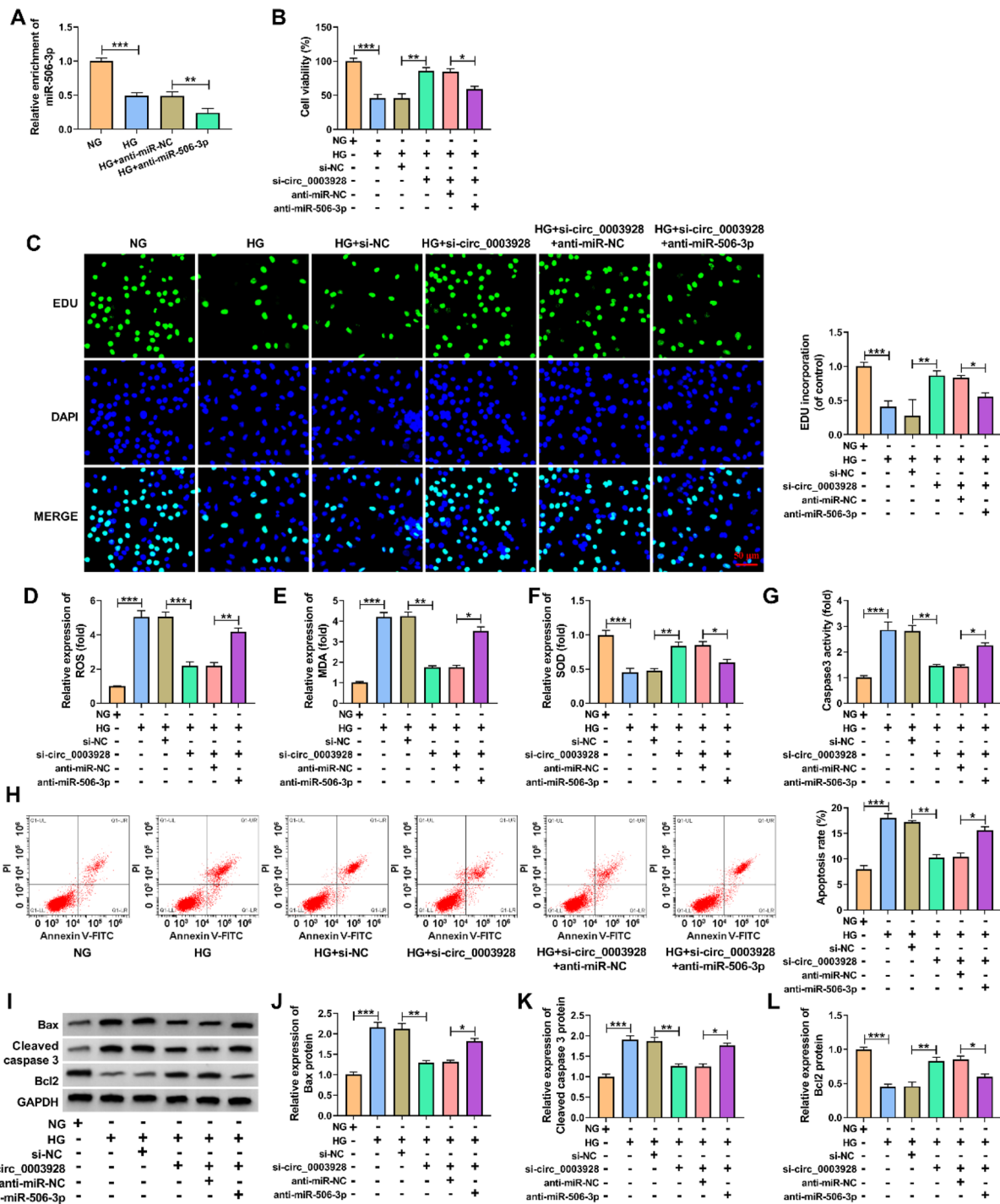


Fig. 5 The effects between circ_0003928 and miR-506-3p on HG-induced oxidative stress and apoptosis of HK-2 cells. **A** MiR-506-3p expression was detected by qRT-PCR in the HK-2 cells treated with NG, HG, anti-miR-NC or anti-miR-506-3p. **B–L** HK-2 cells were treated with NG, HG, HG + si-NC, HG + si-circ_0003928, HG + si-circ_0003928 + anti-miR-NC or HG + si-circ_0003928 + anti-miR-506-3p, and cell viability was analyzed by a CCK-8 assay (**B**), cell proliferation by an EdU assay (**C**), ROS level by a cellular ROS assay kit (**D**), MDA production by a lipid peroxidation MDA assay kit (**E**), SOD activity by a Superoxide dismutase activity assay kit (**F**), caspase 3 activity by a caspase 3 activity assay (**G**), cell apoptotic rate by flow cytometry analysis (**H**), and the protein expression of Bax, cleaved caspase 3 and Bcl 2 by Western blotting analysis (**I–L**). **P* < 0.05, ***P* < 0.01 and ****P* < 0.001

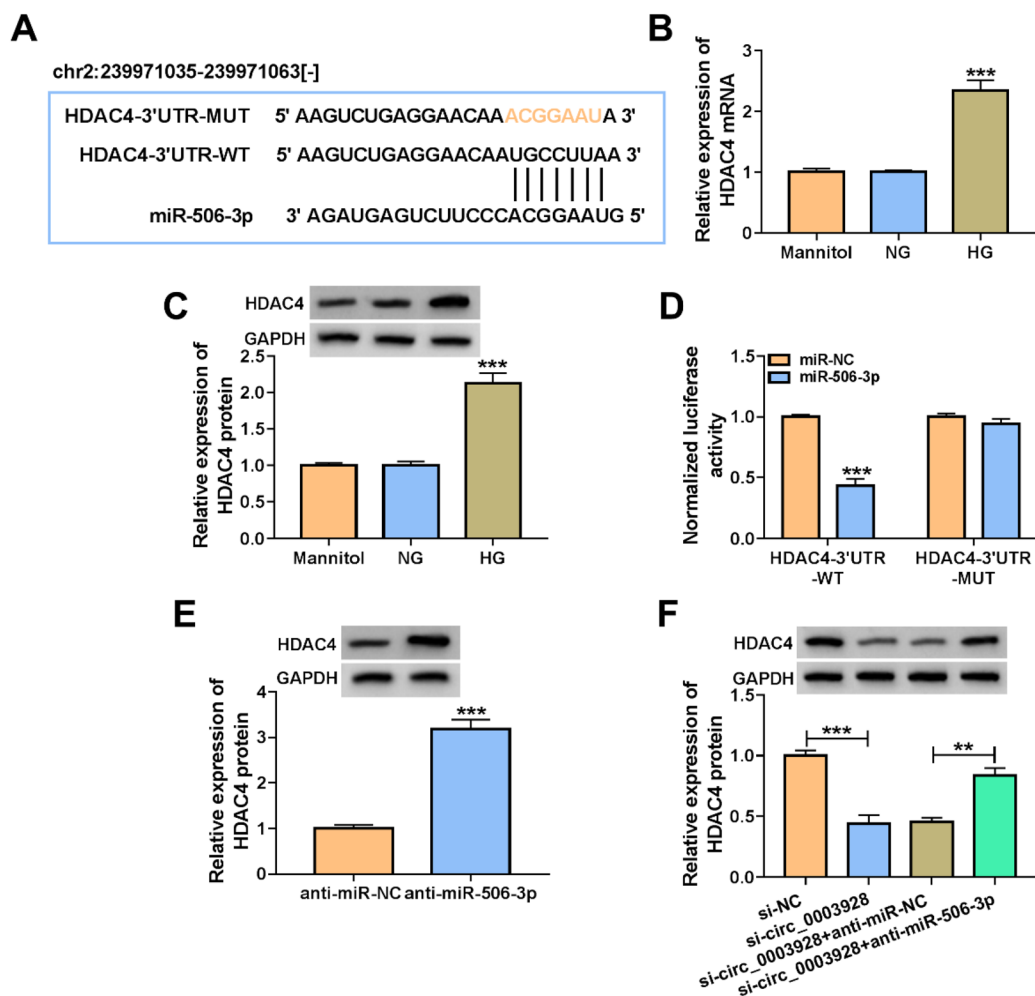


Fig. 6 Circ_0003928 modulated HDAC4 expression through miR-506-3p. **A** The schematic illustration showed the complementary sites of miR-506-3p with HDAC4 3'UTR. **B** and **C** HDAC4 expression was detected by qRT-PCR and Western blotting in the HK-2 cells induced by Mannitol, NG or HG. **D** The dual-luciferase reporter assay was used to determine the interaction of miR-506-3p with HDAC4 3'UTR. **E** The effect of miR-506-3p depletion on HDAC4 protein expression was determined by Western blotting analysis. **F** The effects between circ_0003928 knockdown and miR-506-3p inhibitors on HDAC4 protein expression were analyzed by Western blotting analysis. ** $P < 0.01$ and *** $P < 0.001$

significant difference after transfection with miR-506-3p mimics (Fig. 6D). Consistently, it was found that miR-506-3p inhibitors dramatically increased the HDAC4 expression (Fig. 6E). As revealed by Spearman correlation analysis, miR-506-3p was negatively correlated with HDAC4 expression in serum samples of DN patients (Additional file 2: Figure S2B). The above data demonstrate that HDAC4 is a target gene of miR-506-3p. Based on the above results, we analyzed the regulatory relationship among circ_0003928, miR-506-3p and HDAC4 using Western blotting. As presented in Fig. 6F, circ_0003928 depletion inhibited HDAC4 production, whereas the effect was relieved after miR-506-3p was downregulated. Taken together,

all evidence suggests that circ_0003928 can regulate HDAC4 expression through miR-506-3p.

Circ_0003928 knockdown ameliorated HG-induced HK-2 cell damage through HDAC4

Considering that circ_0003928 could regulate HDAC4 expression by associating with miR-506-3p, we further analyzed whether the inner mechanism of circ_0003928 in mediating HG-caused HK-2 cell damage involved HDAC4. As shown in Fig. 7A, HG treatment significantly promoted HDAC4 production, which was increased after HDAC4 overexpression. Subsequently, circ_0003928 knockdown promoted the viability and proliferation of HG-induced HK-2 cells,

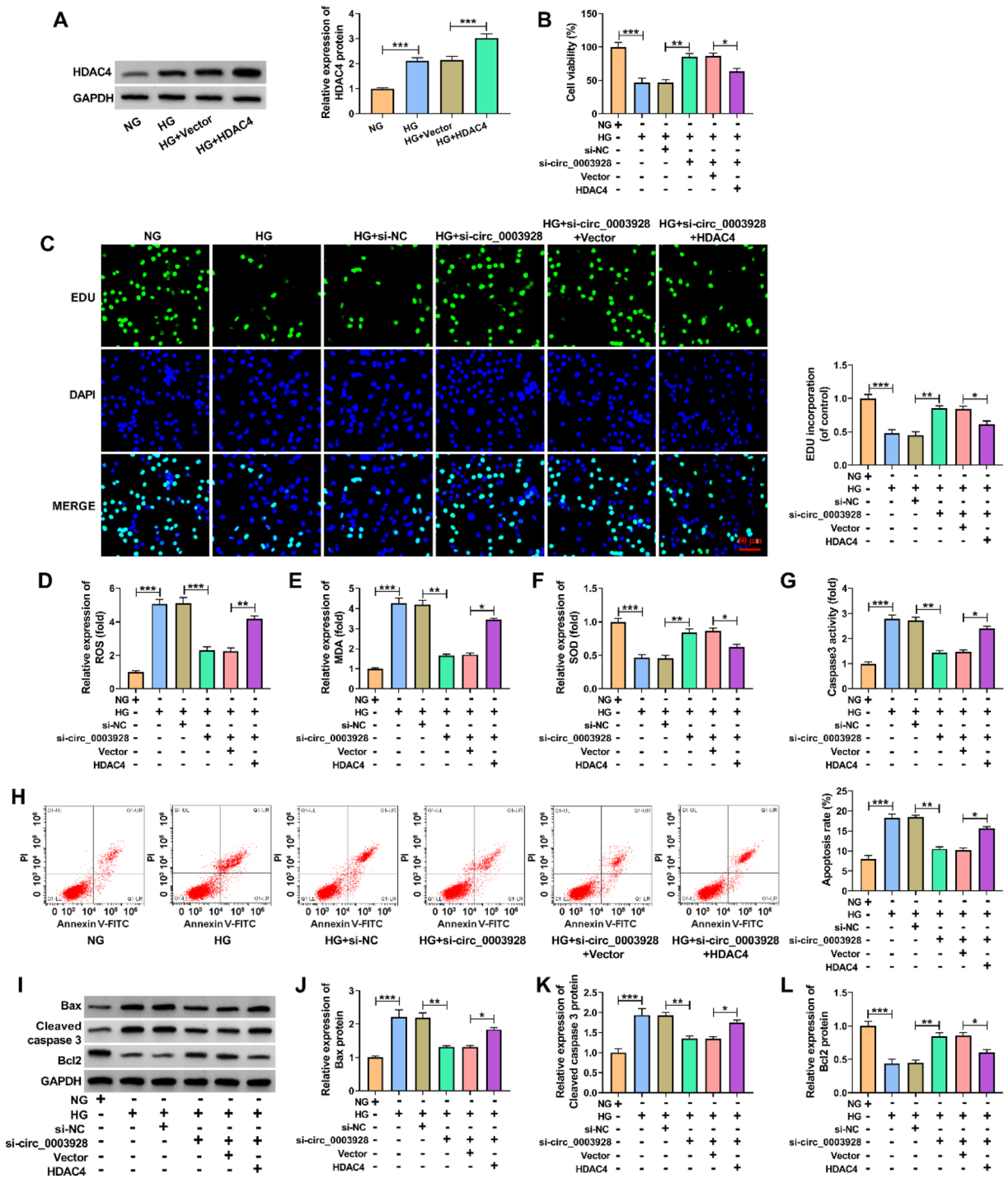


Fig. 7 Circ_0003928 regulated HG-caused HK-2 cell disorders through HDAC4. **A** HDAC4 expression was detected by Western blotting analysis in the HK-2 cells treated with NG, HG, Vector or HDAC4. **B–L** HK-2 cells were treated with NG, HG, HG + si-NC, HG + si-circ_0003928, HG + si-circ_0003928 + Vector or HG + si-circ_0003928 + HDAC4, and cell viability was analyzed by a CCK-8 assay (**B**), cell proliferation by an EdU assay (**C**), ROS level by a cellular ROS assay kit (**D**), MDA production by a lipid peroxidation MDA assay kit (**E**), SOD activity by a Superoxide dismutase activity assay kit (**F**), caspase 3 activity by a caspase 3 activity assay (**G**), cell apoptotic rate by flow cytometry analysis (**H**), and the protein expression of Bax, cleaved caspase 3 and Bcl 2 by Western blotting analysis (**I–L**). **P* < 0.05, ***P* < 0.01 and ****P* < 0.001

which was attenuated after HDAC4 overexpression (Fig. 7B and C). The decreased ROS and MDA production and increased SOD activity by circ_0003928 knockdown were also relieved by the enforced expression of HDAC4 in HG-treated HK-2 cells (Fig. 7D–F). Comparatively, circ_0003928 depletion inhibited caspase 3 activity, cell apoptotic rate and the protein expression of Bax and cleaved caspase 3, and promoted Bcl 2 production in HG-treated HK-2 cells; however, these effects were remitted when HDAC4 expression was increased (Fig. 7G–L). Thus, these results demonstrate that circ_0003928 regulates HG-induced cell disorders through HDAC4.

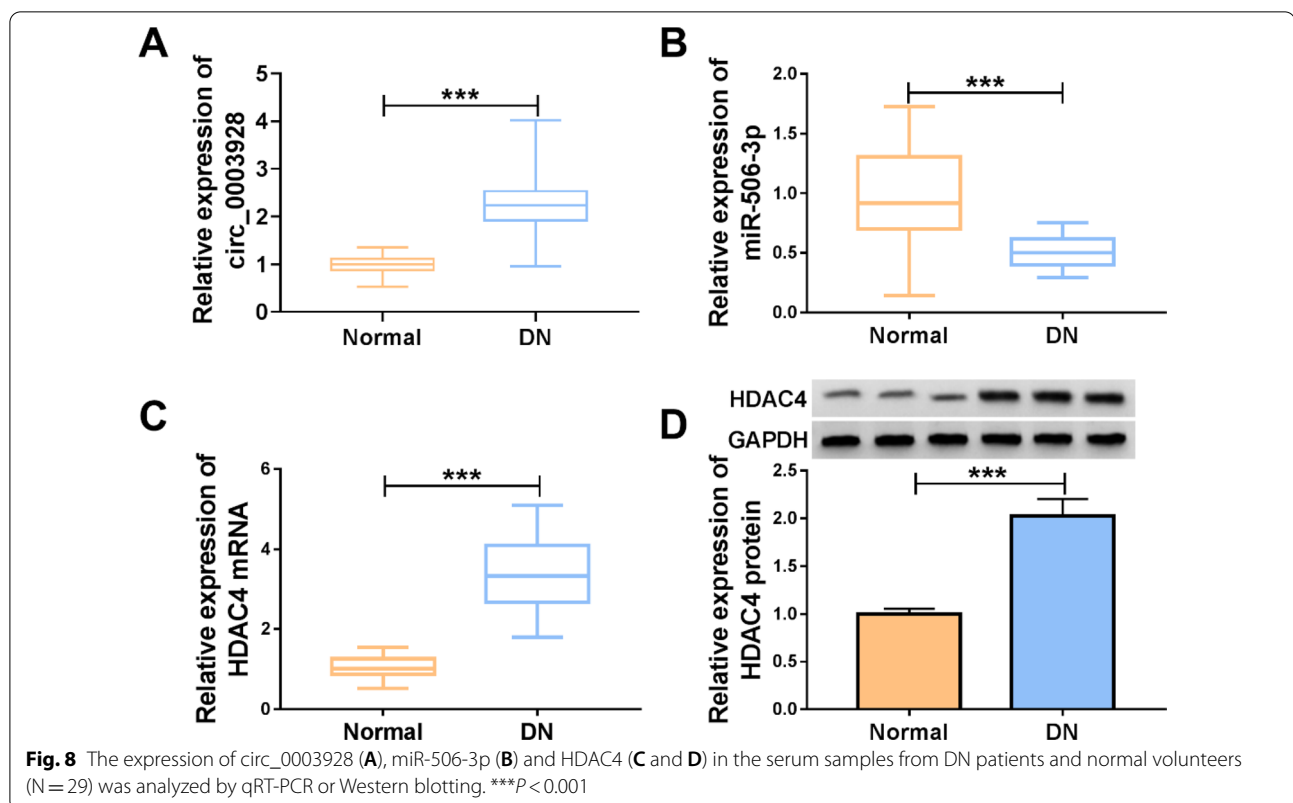
The expression of circ_0003928, miR-506-3p and HDAC4 in the serum samples from DN patients

The study further detected circ_0003928, miR-506-3p and HDAC4 expression in the serum samples from DN patients and healthy volunteers. As shown in Fig. 8A, circ_0003928 was significantly upregulated in the serum samples of DN patients compared with healthy controls. Subsequently, we observed a lower level of miR-506-3p and a high HDAC4 expression in the serum samples of DN patients compared with control groups (Fig. 8B–D).

Discussion

Recently, increasing evidence suggests that circRNAs are involved in the mechanism of DN progression [21]. In the present work, we analyzed the function of circ_0003928 in HG-induced human tubular epithelial cell dysfunction and disclosed the underlying mechanism. As a result, we found that circ_0003928 participated in regulating proliferation, oxidative stress and apoptosis of HG-treated human tubular epithelial cells through the miR-506-3p/HDAC4 pathway.

TAOK1, a parental gene of circ_0003928, is a member of human TAO kinase orthologs (TAOKs) that participate in multiple signaling pathways, such as the JNK/SAPK cascade, the p38 MAPK pathway and the Hippo signaling pathway [22]. Through these interactions, TAOKs regulate cytoskeleton, inflammatory response, oxidative stress and apoptosis and other cellular pathways [3]. Oxidative stress is regarded as an important factor associated with hyperglycemia [3]. Hyperglycemia accelerates apoptosis of different cells, such as tubular epithelial cells and endothelial cells, through activation of some signaling pathways, leading to renal injury in DN [23, 24]. In this work, we analyzed the role of circ_0003928 in HG-caused oxidative stress and apoptosis of human tubular epithelial cells. Herein, we found a high expression of circ_0003928 in the serum of DN patients and



HG-treated human tubular epithelial cells, and the promoting effect of circ_0003928 on HK-2 cell apoptosis, which were consistent with the published data [18]. In addition, the work provided evidence that circ_0003928 silencing attenuated HG-induced proliferation inhibition and oxidative stress promotion.

miRNA is a short noncoding RNA that has attracted much attention as an important regulator of DN progression [25]. Considerable studies suggest that circRNA contains the complementary sites of miRNA, and combines with miRNA [26]. Herein, we found that miR-506-3p combined with circ_0003928. As reported early, miR-506-3p regulates the progression of cancer [27], atherosclerosis [28], bronchial asthma [29] and cardiovascular disease [30]. In particular, miR-506-3p combined with long noncoding RNA KCNQ1OT1 (lncRNA KCNQ1OT1) to regulate HK-2 cell oxidative stress and pyroptosis [17]. The present study suggested that miR-506-3p promoted HK-2 cell proliferation. Besides, miR-506-3p inhibited HK-2 cell oxidative stress and apoptosis. Importantly, we provided evidence that circ_0003928 regulated HG-induced HK-2 cell dysfunction through miR-506-3p.

The HDAC family is a class of enzymes able to modulate acetylation activities of histone acetyltransferases, playing important parts in mediating gene transcription [31]. There are data suggesting the involvement of the HDAC family in DN progression through various molecular pathways [32]. Among several HDACs, HDAC4 is highly expressed in DN and is a major contributor to podocytes' injury [33]. Mechanistically, HDAC4 contributes to podocyte dysfunction through several mechanisms, such as interacting with miR-29a [34] and upregulating calcineurin [35]. In the present investigation, HDAC4 was associated with miR-506-3p. HDAC4 was highly expressed in DN patients and HG-induced HK-2 cell samples. Besides, HDAC4 overexpression attenuated circ_0003928 depletion-mediated effects in HG-induced HK-2 cells. Further, circ_0003928 negatively regulated miR-506-3p to promote HDAC4 production.

Conclusion

Taken together, the present study demonstrates that circ_0003928 is a crucial regulator of the signal transduction pathway related to HG-induced HK-2 cell dysfunction in DN. HG-induced HK-2 cell injury involved the upregulation of circ_0003928. The increased expression of circ_0003928 induced HDAC4 production by sponging miR-506-3p, further inhibiting cell proliferation and promoting oxidative stress and cell apoptosis (Additional file 3: Figure S3). Interfering the circ_0003928/miR-506-3p/HDAC4 axis may be an effective method for the therapy of DN. Besides,

tubular epithelial cell-specific circ_0003928 knock-down diabetic db/db mice will be an ideal model for analyzing the role of circ_0003928 in DN in vivo. Thus, our findings will be further testified in subsequent investigations using the genetic model. Previous studies have shown that the Nrf2/heme oxygenase-1 (HO-1) pathway regulates diabete-caused kidney damage [36], and that miR-505-3p aggravates oxidative stress injury through the Nrf2/HO-1 signaling pathway [37]. Thus, whether circ_0003928-mediated HK-2 cell dysfunction involves the pathway will be explored in the future.

Supplementary Information

The online version contains supplementary material available at <https://doi.org/10.1186/s40001-022-00679-y>.

Additional file 1: Figure S1. Circ_0003928-associated miRNAs and miR-506-3p-associated mRNAs were analyzed by qRT-PCR in HK-2 cells. * $P < 0.05$, ** $P < 0.01$ and *** $P < 0.001$.

Additional file 2: Figure S2. Spearman correlation analysis was performed to determine the correlation between miR-506-3p and circ_0003928 (A) or HDAC4 (B) in the serum samples of DN patients.

Additional file 3: Figure S3. The schematic illustration showed the mechanism by which circ_0003928 regulated HG-induced HK-2 cell dysfunction. HG-induced HK-2 cell injury involved the upregulation of circ_0003928. The increased expression of circ_0003928 induced HDAC4 production by sponging miR-506-3p, further inhibiting cell proliferation and promoting oxidative stress and cell apoptosis.

Acknowledgements

None.

Authors' contributions

CZ designed and supervised the study. QL conducted the experiments and drafted the manuscript. ND collected and analyzed the data. YC contributed the methodology and edited the manuscript. All authors read and approved the final manuscript.

Funding

None.

Availability of data and materials

The analyzed data sets generated during the study are available from the corresponding author on reasonable request.

Declarations

Ethics approval and consent to participate

The clinical trial obtained approval from the Ethics Committee of Hebei General Hospital and was carried out according to the guidelines of Declaration of Helsinki.

Consent for publication

Not applicable.

Competing interests

The authors report no conflicts of interest.

Author details

¹Department of Nephrology, Hebei General Hospital, Shijiazhuang, China.

²Department of Endocrine Rheumatology and Immunology, People's Hospital of Gaotang County, Gaotang, China. ³Department of Clinical Laboratory, Hebei General Hospital, Shijiazhuang, China. ⁴Department of Kidney Internal

Medicine, Zaozhuang Municipal Hospital, No. 41 Longtou Road, Central District, Zaozhuang 277100, China.

Received: 10 January 2022 Accepted: 20 March 2022

Published online: 07 April 2022

References

- Yamahara K, Yasuda M, Kume S, Koya D, Maegawa H, Uzu T. The role of autophagy in the pathogenesis of diabetic nephropathy. *J Diabetes Res*. 2013;2013:193757.
- Najafian B, Alpers CE, Fogo AB. Pathology of human diabetic nephropathy. *Contrib Nephrol*. 2011;170:36–47.
- Sifuentes-Franco S, Padilla-Tejeda DE, Carrillo-Ibarra S, Miranda-Díaz AG. Oxidative stress, apoptosis, and mitochondrial function in diabetic nephropathy. *Int J Endocrinol*. 2018;2018:1875870–1875870.
- Dröge W. Free radicals in the physiological control of cell function. *Physiol Rev*. 2002;82(1):47–95.
- Danan M, Schwartz S, Edelheit S, Sorek R. Transcriptome-wide discovery of circular RNAs in *Archaea*. *Nucleic Acids Res*. 2012;40(7):3131–42.
- Bach DH, Lee SK, Sood AK. Circular RNAs in Cancer. *Mol Ther Nucleic Acids*. 2019;16:118–29.
- Kristensen LS, Andersen MS, Stagsted LVW, Ebbesen KK, Hansen TB, Kjems J. The biogenesis, biology and characterization of circular RNAs. *Nat Rev Genet*. 2019;20(11):675–91.
- Jin J, Sun H, Shi C, Yang H, Wu Y, Li W, et al. Circular RNA in renal diseases. *J Cell Mol Med*. 2020;24(12):6523–33.
- Peng F, Gong W, Li S, Yin B, Zhao C, Liu W, et al. circRNA_010383 acts as a sponge for miR-135a and its downregulated expression contributes to renal fibrosis in diabetic nephropathy. *Diabetes*. 2020;70(2):603–15.
- Ge X, Xi L, Wang Q, Li H, Xia L, Cang Z, et al. Circular RNA Circ_0000064 promotes the proliferation and fibrosis of mesangial cells via miR-143 in diabetic nephropathy. *Gene*. 2020;758:144952.
- Jin G, Wang Q, Hu X, Li X, Pei X, Xu E, et al. Profiling and functional analysis of differentially expressed circular RNAs in high glucose-induced human umbilical vein endothelial cells. *FEBS Open Bio*. 2019;9(9):1640–51.
- Aravindan N, Subramanian K, Somasundaram DB, Herman TS, Aravindan S. MicroRNAs in neuroblastoma tumorigenesis, therapy resistance, and disease evolution. *Cancer Drug Resist*. 2019;2:1086–105.
- Jiang ZH, Tang YZ, Song HN, Yang M, Li B, Ni CL. miRNA-342 suppresses renal interstitial fibrosis in diabetic nephropathy by targeting SOX6. *Int J Mol Med*. 2020;45(1):45–52.
- Zhao SM, Zhang T, Qiu Q, Xu C, Ma LJ, Liu J, et al. MiRNA-337 leads to podocyte injury in mice with diabetic nephropathy. *Eur Rev Med Pharmacol Sci*. 2019;23(19):8485–92.
- Li A, Peng R, Sun Y, Liu H, Peng H, Zhang Z. LincRNA 170002014Rik alleviates cell proliferation and fibrosis in diabetic nephropathy via miR-34a-5p/Sirt1/HIF-1 α signaling. *Cell Death Dis*. 2018;9(5):461.
- Salmena L, Poliseno L, Tay Y, Kats L, Pandolfi PP. A ceRNA hypothesis: the Rosetta Stone of a hidden RNA language?. *Cell*. 2011; 146(3):353–358.
- Zhu B, Cheng X, Jiang Y, Cheng M, Chen L, Bao J, et al. Silencing of KCNQ10T1 decreases oxidative stress and pyroptosis of renal tubular epithelial cells. *Diabetes Metab Syndr Obes*. 2020;13:365–75.
- An L, Ji D, Hu W, Wang J, Jin X, Qu Y, et al. Interference of Hsa_circ_0003928 alleviates high glucose-induced cell apoptosis and inflammation in HK-2 Cells via miR-151-3p/Anxa2. *Diabetes Metab Syndr Obes*. 2020;13:3157–68.
- Barber RD, Harmer DW, Coleman RA, Clark BJ. GAPDH as a housekeeping gene: analysis of GAPDH mRNA expression in a panel of 72 human tissues. *Physiol Genomics*. 2005;21(3):389–95.
- Mou X, Chen JW, Zhou DY, Liu K, Chen LJ, Zhou D, et al. A novel identified circular RNA, circ_0000491, aggravates the extracellular matrix of diabetic nephropathy glomerular mesangial cells through suppressing miR-101b by targeting TGF β R1. *Mol Med Rep*. 2020;22(5):3785–94.
- Lv J, Wu Y, Mai Y, Bu S. Noncoding RNAs in diabetic nephropathy: pathogenesis, biomarkers, and therapy. *J Diabetes Res*. 2020;2020:3960857–3960857.
- Fang CY, Lai TC, Hsiao M, Chang YC. The diverse roles of TAO kinases in health and diseases. *Int J Mol Sci*. 2020;21(20):7463.
- Simone S, Gorin Y, Velagapudi C, Abboud HE, Habib SL. Mechanism of oxidative DNA damage in diabetes: tuberin inactivation and downregulation of DNA repair enzyme 8-oxo-7,8-dihydro-2'-deoxyguanosine-DNA glycosylase. *Diabetes*. 2008;57(10):2626–36.
- Adeghate E. Molecular and cellular basis of the aetiology and management of diabetic cardiomyopathy: a short review. *Mol Cell Biochem*. 2004;261(1–2):187–91.
- Ishii H, Kaneko S, Yanai K, Aomatsu A, Hirai K, Ookawara S, et al. MicroRNAs in podocyte injury in diabetic nephropathy. *Front Genet*. 2020;11:993–993.
- Panda AC. Circular RNAs Act as miRNA Sponges. *Adv Exp Med Biol*. 2018;1087:67–79.
- Shang A, Gu C, Wang W, Wang X, Sun J, Zeng B, et al. Exosomal circ-PACRGL promotes progression of colorectal cancer via the miR-142-3p/miR-506-3p-TGF- β 1 axis. *Mol Cancer*. 2020;19(1):117.
- Dong H, Jiang G, Zhang J, Kang Y. MiR-506-3p promotes the proliferation and migration of vascular smooth muscle cells via targeting KLF4. *Pathobiology*. 2021;88(4):277–88.
- Manli W, Hua Q. Effect of miR-506-3p on proliferation and apoptosis of airway smooth muscle cells in asthmatic mice by regulating CCL2 gene expression and mediating TLR4/NF- κ B signaling pathway activation. *Mol Biotechnol*. 2021;63(5):410–23.
- Yi F, Hao Y, Chong X, Zhong W. Overexpression of microRNA-506-3p aggravates the injury of vascular endothelial cells in patients with hypertension by downregulating Beclin1 expression. *Exp Ther Med*. 2018;15(3):2844–50.
- Pang M, Zhuang S. Histone deacetylase: a potential therapeutic target for fibrotic disorders. *J Pharmacol Exp Ther*. 2010;335(2):266–72.
- Khullar M, Cheema BS, Raut SK. Emerging evidence of epigenetic modifications in vascular complication of diabetes. *Front Endocrinol (Lausanne)*. 2017;8:237.
- Wang X, Liu J, Zhen J, Zhang C, Wan Q, Liu G, et al. Histone deacetylase 4 selectively contributes to podocyte injury in diabetic nephropathy. *Kidney Int*. 2014;86(4):712–25.
- Lin CL, Lee PH, Hsu YC, Lei CC, Ko JY, Chuang PC, et al. MicroRNA-29a promotion of nephrin acetylation ameliorates hyperglycemia-induced podocyte dysfunction. *J Am Soc Nephrol*. 2014;25(8):1698–709.
- Shi W, Huang Y, Zhao X, Xie Z, Dong W, Li R, et al. Histone deacetylase 4 mediates high glucose-induced podocyte apoptosis via upregulation of calcineurin. *Biochem Biophys Res Commun*. 2020;533(4):1061–8.
- Ma H, Wang X, Zhang W, Li H, Zhao W, Sun J, et al. Melatonin Suppresses Ferroptosis induced by high glucose via activation of the Nrf2/HO-1 Signaling pathway in type 2 diabetic osteoporosis. *Oxid Med Cell Longev*. 2020;2020:9067610–9067610.
- Tang M, Zhang L, Zhu Z, Li R, Wang S, Wang W, et al. Overexpression of miR-506-3p Aggravates DBP-induced testicular oxidative stress in rats by downregulating ANXA5 via Nrf2/HO-1 Signaling Pathway. *Oxid Med Cell Longev*. 2020;2020:4640605.

Publisher's Note

Springer Nature remains neutral with regard to jurisdictional claims in published maps and institutional affiliations.

Ready to submit your research? Choose BMC and benefit from:

- fast, convenient online submission
- thorough peer review by experienced researchers in your field
- rapid publication on acceptance
- support for research data, including large and complex data types
- gold Open Access which fosters wider collaboration and increased citations
- maximum visibility for your research: over 100M website views per year

At BMC, research is always in progress.

Learn more biomedcentral.com/submissions

